APPLIED ORGANOMETALLIC CHEMISTRY
Appl. Organometal. Chem. 2001; **15**: 841–857
DOI: 10.1002/aoc.239

Synthesis of Si–C–N coatings by thermal Plasmajet chemical vapour deposition applying liquid precursors

Johannes Wilden,[1]* Andreas Wank,[1] Marcus Asmann,[2]
Joachim V. R. Heberlein,[2] Maher I. Boulos[3] and Francois Gitzhofer[3]
[1]Institute of Composite Materials, Chemnitz University of Technology, 09107 Chemnitz, Germany
[2]Institute of Technology, University of Minnesota, Minneapolis, MN, USA
[3]Plasma Technology Research Centre, University of Sherbrooke, Sherbrooke, Quebec, Canada

Materials in the system Si–C–N feature excellent properties for wear protection applications, even at elevated temperatures, and an excellent thermal shock resistance. As these materials have no melting point, coatings have to be manufactured via a synthesis. Conventional chemical vapour deposition (CVD) processes have the disadvantage of low deposition rates. Thermal Plasmajet CVD processes with liquid feedstock feature the highest deposition rates among the gas-phase synthesis processes. Single and triple DC torches and HF torches with supersonic nozzles have successfully been applied to produce Si–C(–N) coatings on different steel, aluminium, titanium and copper alloys, as well as on graphite. Besides chlorosilanes, hexamethyldisiloxane, tetramethyldisiloxane and hexamethyldisilazane have been used as liquid single precursors. Deposition rates up to 1500 μm h^{-1} have been achieved. The coatings show cauliflower, columnar or dense morphology and an amorphous or nanocrystalline structure. The formation of both α- and β-Si_3N_4 has been verified by X-ray diffraction. The application of chlorosilanes always results in chlorine-containing coatings. The chlorine causes severe corrosion in the interface to mild carbon steel substrates. The processes are compared taking into account their characteristics concerning the injection modes, gas temperature and velocity profiles determined by enthalpy probe measurements. The process conditions are correlated to the coating microstructure and the adhesion to the substrates and guidelines for the optimum production of Si–C–N coatings by Plasmajet CVD are deduced. Emission spectroscopy is used to determine the mechanisms of the coating formation. Full dissociation of the liquid feedstock in the plasma jet has been verified. Copyright © 2001 John Wiley & Sons, Ltd.

Keywords: TPCVD; thermal plasma; DC Plasmajet CVD; HF plasma; plasma diagnostics; SiC; Si_3N_4; liquid precursor; supersonic; high rate synthesis

Received 15 February 2001; accepted 26 March 2001

1 INTRODUCTION

Silicon carbide (SiC) is a material with excellent properties for wear and high-temperature oxidation protection applications. Besides a hardness of 3500 HV and a high heat conductivity (100 W m^{-1} K^{-1} at ambient temperature; 25 W m^{-1} K^{-1} at 1400°C), it shows good resistance against corrosion and oxidation, even at high temperatures. Furthermore, SiC is a lightweight material with a theoretical density of 3.2 g cm^{-3}. There is a particular interest in SiC coatings for protection of various substrate materials. Conventional coating technologies for production of pure, thick SiC coatings, like thermal spraying or welding, cannot be applied, as SiC has no liquid phase; it disintegrates at high temperatures.

In general, these days non-equilibrium plasma processes are applied to grow silicon carbide coatings. However, these processes are comparatively time demanding when thick coatings (>15 μm) are needed, and, therefore, often do not

* Correspondence to: J. Wilden, Institute of Composite Materials, Chemnitz University of Technology, Chemnitz, Germany.
Email: johannes.wilden@mbv.tu-chemnitz.de
Contract/grant sponsor: Deutsche Forschungsgemeinschaft; Contract/grant number: SPP 1037; Contract/grant number: Wi 1509/2.

fit the logistical and economic demands of industrial processes. In contrast thermal Plasmajet chemical vapour deposition (TPCVD) processes are known for their comparatively high deposition rates. For example, the growth rate of diamond coatings in TPCVD processes can exceed 100 $\mu m\ h^{-1}$.

2 PROCESSES FOR SiC SYNTHESIS

2.1 Conventional thick coating technologies

Conventional thermal spray technologies use solid-state feedstock in rod or powder shape. However, these technologies do not permit manufacture of pure SiC coatings, because there is no SiC liquid phase and its ductility is too low for compaction of particles on the substrate surface at temperatures below its disintegration temperature. Depending on the environment, degradation starts at 1800°C.

There has been considerable effort to produce SiC-containing cermet coatings with various metallic binders, because, in addition to its outstanding properties, SiC is a comparatively cheap material. Until now, however, all approaches have shown only minor success, because of the high tendency of SiC to dissolve in the metallic binders. This leads to low carbide particle contents and the formation of brittle silicide phases, which result in poor wear behaviour for the coatings. To produce coatings with a high SiC content the particles have to be covered completely by a metallic binder; this provides sufficient ductility at temperatures significantly below the SiC disintegration temperature and at the temperature at which interaction of the metallic binder with SiC becomes a problem. There are chemical processes that are capable of producing such coated SiC particles, but they are very time consuming and expensive. To meet the process characteristic demands, low temperature and high velocity spraying technologies have to be applied. As yet there are no industrial applications for SiC-containing cermet coatings.

2.2 Thin coating technologies

All thin coating technologies have in common that they are synthesis processes, which means that the SiC coating is formed by a chemical reaction. In most processes the gaseous state of the precursors is included, at least as an intermediate step.

Various precursors can be applied. Reactive physical vapour deposition (PVD) processes use silicon targets and a carburizing reactive gas like methane or acetylene.[1] In the various CVD processes, vaporized liquids, like hexamethyldisilane ($(CH_3)_3Si_2(CH_3)_3$), tetrachlorosilane ($SiCl_4$) or naturally gaseous precursors like silane (SiH_4), in combination with a carbon precursor are applied. The most common silicon sources, SiH_4 and $SiCl_4$, are quite hazardous. SiH_4 is poisonous, highly explosive and self-flammable at ambient conditions. So there are high demands on mechanisms for personal protection when SiH_4 is applied. Additionally, coatings synthesized from SiH_4 are likely to show a high content of Si—H bonds; these affect the coatings properties, including their thermal stability. Chlorine-containing precursors, like $SiCl_4$, also require attention to personal and machinery protection, because of their corrosive nature. Furthermore, even small impurity contents of chlorine can destroy the compound by corrosion reactions at the interface with the substrate.

Another characteristic of thin coating technologies is a low deposition rate and, therefore, a comparatively long production cycle. However, these processes have also been proven to be capable of producing coatings with the highest quality features concerned with purity, homogeneity, density and crystal structure; even epitaxial coatings can be produced.

2.2.1 Thermal CVD

In these processes, the substrate surface acts as a catalyst for a chemical reaction. The activation energy for the reaction is provided by raising the temperature. In the early stage of coating formation, nuclei develop on the substrate surface, grow to a critical size by surface diffusion of the reacting species and become stable. Not every substrate material permits the necessary processing temperatures and, depending on the reactivity between the substrate and coating material, the interface can be damaged severely. Usually the deposition temperatures exceed 800°C.

For example, SiH_2Cl_2, C_4H_{10} and hydrogen can be used as precursors of a thermal CVD process at ambient pressure and 1500 K.[2] Furthermore, for the production of Si—C—N coatings, processes using $Si(CH_3)_4$ and ammonia, and substrate temperatures exceeding 1000°C are necessary; and for the application of several single precursors, in metal-

loorganic CVD processes minimum substrate temperatures of 750°C are reported.[3–6]

2.2.2 Plasma-enhanced CVD (PECVD) processes

In this section, the processes using non-equilibrium plasmas are discussed. Non-equilibrium plasmas are characterized by a strong difference in the temperature of the free electrons T_e, and heavy particles T_h, i.e. ions or excited atoms, at the same location ($T_e \gg T_h$).

There are a variety of plasma-assisted CVD processes. They all have in common the use of a discharge to excite process gases, which interact with the reactants that form the coating, or to excite the reactants themselves. The direct interaction with the reactants is energetically more efficient and, therefore, allows higher deposition rates. For a remote plasma CVD process, using the precursor hexamethyldisilane, deposition rates lower than $2\ nm\ h^{-1}$ are reported.[7] However, the coatings manufactured in this process show a perfect interface between substrate and surface, because there is no bombardment of electrons or heavy particles, as in processes that use a plasma on the substrate surface. Additionally, a significant improvement concerning the homogeneity of the coatings thickness distribution is achieved.

The additional energy transfer to the reactants allows lower substrate temperatures. Usually 200 to 400°C is sufficient,[8–12] and for remote plasmas the substrate temperatures can be kept at 30°C.[7] However, when a silicon precursor with bonds between silicon and hydrogen is applied, low substrate temperatures favour the transfer of hydrogen into the coating structure, which leads to inferior mechanical properties. For coatings manufactured from SiH_4 and different carbon precursors, hydrogen contents up to 41 at.% are reported.[8] These coatings show considerable compressive residual stresses, but annealing treatments, which cause hydrogen evolution, can result in complete relaxation or even the development of tensile residual stresses.[10] The more the residual stresses change to tensile, the more the adhesive and cohesive strength of the coatings, and subsequently the wear resistance, is reduced. The changes of the coatings properties have to be considered carefully when PECVD SiC coatings are applied at elevated temperatures.

PECVD SiC coatings show a fracture toughness comparable to CVD TiN coatings ($4\ MPa\ m^{0.5}$), and the corrosion resistance is improved by three orders of magnitude.[12] Therefore, these coatings show outstanding performance in combined wear and corrosion protection applications. The hardness depends substantially on the coatings stoichiometry. In particular, an excess of carbon results in a steep hardness decrease.[9] But as the carbon may work as a lubricant in some wear cases, the loss of hardness might be balanced by the decrease of friction.

2.2.3 Special coating technologies

There is a variety of other technologies, that can be used to produce SiC coatings. For example, a reactive PVD process can be used, in which a solid silicon target acts as silicon source and a reactive gas, like methane or acetylene, as a carbon source. Because SiC has high electrical conductivity, SiC sputter targets can also be used. In such sputtering processes, the substrate temperatures are usually between 350 and 450°C and deposition rates amount to $1.5\ \mu m\ h^{-1}$. Even at these low substrate temperatures, interface damage occurs in high-speed steel substrates due to the Kirkendall effect.[1]

A photochemical CVD process using Si_2H_6 and CCl_4 as precursors is known to produce very thin coatings with outstanding quality with regard to lattice defects and low interface damage, as, in contrast to PECVD processes, there is no ion bombardment. Deposition rates of $20\ nm\ h^{-1}$ can be achieved.[13] Laser-assisted methods are usually applied in the field of powder production.[14–18]

Furthermore, dip-coating processes can be applied; these are based on the wetting and physical adsorption of a liquid precursor into which a substrate is submerged. During a heat treatment, the precursor is pyrolysed and the SiC coating is formed. Coatings with thickness of about 1 μm per immersion can be obtained, and the coatings show high residual stresses due to shrinkage during pyrolysis. To increase the coating thickness, the procedure can be repeated several times.

The polymer-spraying process is comparable to the dip-coating process, but the liquid precursor, which is already to some extent polymerized, is sprayed onto the substrate by varnishing equipment. In a polymerization and pyrolysis heat treatment, SiC forms. Depending on the initial grade of polymerization, coatings with a homogeneous thickness distribution and low porosity can be manufactured. The critical thickness to avoid formation of cracks, when coating alumina, silicon wafers, graphite or SiC, is 2.5 μm for Si–C–O coatings and 1 μm for Si–C–N coatings. These coatings have been proven to be suitable for sealing substrate surfaces with open porosity.[19]

2.3 TPCVD processes

In this section the plasma processes with a partial local thermodynamic equilibrium are described. In these plasmas, the temperatures of the free electrons T_e, and the heavy particles T_h, i.e. ions or excited atoms, at the same location are about the same ($T_e \approx T_h$).

2.3.1 DC Plasmajet CVD

DC plasma jets are generated by a gas stream passing through an electric arc. Most commonly the gases argon, hydrogen, helium and nitrogen in different mixtures are applied, but systems also working with water vapour or compressed, dry air are available. The arc forms between a tungsten rod cathode and a copper anode — in many cases with a tungsten core, which also acts as nozzle owing to its distinct shape. Both electrodes are water cooled to prevent destruction caused by the heat of the arc. In conventional single cathode torches, the arc rotates on the inner wall of the anode because of a swirling gas stream, which results in a homogeneously shaped jet. The gas passing the arc is excited, mostly dissociated in the case of molecular gases, and partially ionized. The recombination of ionized atoms with free electrons and recombination to molecules at the nozzle exit results in a gas stream with high temperature and high velocity. Temperatures can exceed 15 000 K and the gas velocity can exceed Mach 3, depending on the nozzle shape.

Because of the torch design, axial feeding of reactants separately from the plasma gases is not possible for most available torches. Therefore, the precursors of the Plasmajet CVD process are injected radially at one or more positions at the nozzle exit or further downstream. To control the atmosphere, the process is carried out in a vacuum chamber. Depending on the distance between torch and substrate and the applied substrate material, cooling of the substrate might be necessary to avoid melting and keep the substrate temperature constant. The precursors are injected into the plasma jet, decomposed into their atomic components and excited or even ionized. The homogeneity of the distribution of the atomic components depends substantially on the injection conditions. The best homogeneity is achieved when gaseous precursors are injected together with the plasma gases, but this entails chemical reactions with the electrode material and, therefore, the possibility of electrode degradation and the consumption of reactive species.[20] The atomic species approach the substrate surface and form the coating gradually.

DC plasma jets have been used successfully to synthesize diamond coatings,[21] especially on hard-metal turning tools. Additionally, these jets have been applied to produce nanosized SiC powders from rice hulls.[22] Nanosized powders have proven to result in ceramic components with superior mechanical, physical and/or chemical properties. The size of the powders depends on the quenching rate.[23] A characteristic of thermal plasmas is to provide very steep temperature gradients, and thereby high cooling rates.

SiC coatings have been deposited successfully on graphite and carbon-fibre-reinforced carbon substrates by DC plasma jet CVD with $SiCl_4$ and methane as precursor gases.[20] The coatings show a columnar morphology and the deposition rate is highest in the centre, because the density of atomic species drops from the plasma axis to the fringe. The coating structure and its chemical composition also vary depending on the location of the substrate in the plasma stream.

2.3.2 Triple torch DC Plasmajet CVD

The triple torch DC Plasmajet CVD process works on the same principle as conventional DC Plasmajet CVD processes, but uses three plasma torches with intersecting axes. The torches are angled towards a central injection probe (CIP), which is water cooled, carrying an atomization gas and an inner tube, through which the precursor is fed. In this system, the precursor is atomized into the centre of the converging jet region. As in conventional DC Plasmajet CVD processes, the atmosphere is controlled. Because the triple torch setup is comparatively heavy and bulky, the substrate is moved relative to the torches. The substrate temperature is kept constant by using a water-cooled substrate holder.

As this process features a homogeneous distribution of precursor species inside the converging plasma jet, it is very suitable for production of coatings with high quality with respect to the homogeneity of chemical composition, morphology and structure.

2.3.3 Hypersonic plasma particle deposition (HPPD)

The HPPD process uses a plasma generated by a DC torch, into which gaseous reactants are injected. The mixture is subsequently quenched by supersonic expansion through a nozzle into a vacuum deposition chamber. The high quenching rates cause the nucleation and growth of nanosized particles from the supersaturated vapour. As the

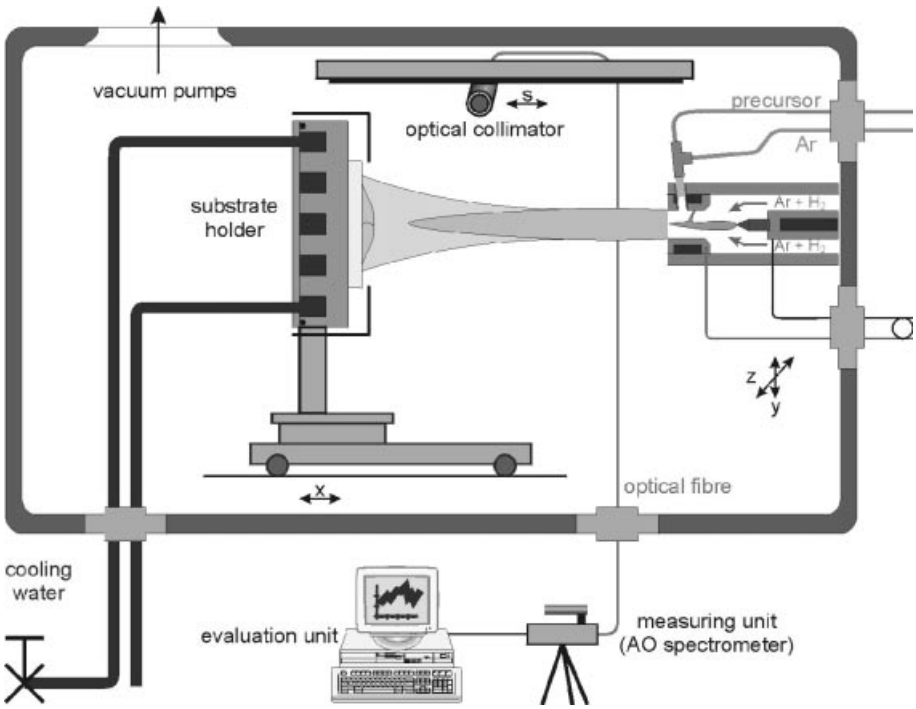

Figure 1 System schematic of the DC Plasmajet CVD process setup.

process is carried out at pressures of about 1 hPa, the particles are accelerated strongly and deposited on the surface of a cooled substrate. The inertial impact with velocities exceeding 1 km s^{-1} results in direct consolidation of the coating without the necessity for further treatment, although subsequent processing may improve the properties of the coating.[24]

This process has been applied successfully to produce silicon and SiC coatings with deposition rates of 3600 μm h^{-1} and 1500 μm h^{-1} respectively.[25] Measurements of the particle size in-flight and the grain size inside the coating showed good agreement, with a mean size of about 10 nm. When the nanosized particles are focused to a narrow beam, which can, for example, be achieved by the application of a system of aerodynamic lenses, this process can also be used to produce nanostructured devices. For example, the production of SiC towers with a diameter below 100 nm and heights exceeding 1 mm have been reported.

2.3.4 HF Plasmajet CVD

HF plasma jets are generated by transferring energy into a gas stream by inductive coupling. Unlike in DC plasma jet generation, there is no contact between the generating components and the plasma gases, which prevents impurities from the electrode material entering the jet. Additionally, the choice of plasma gases does not affect the lifetime of the generating components. In addition to argon, hydrogen, helium and nitrogen, also air and oxygen are conventionally used—the latter especially for production of oxide ceramic coatings. In addition to a separation of plasma gases and carrier gases for the precursor, there is an internal separation of sheath gas and central gas inside the torch. In the centre of the torch a water-cooled central injection probe (CIP) is mounted to allow axial feeding of the precursors inside the torch. Through a quartz tube surrounding the CIP a swirl central gas stream is injected, while the sheath gas, which is also used to cool the ceramic tube wall, is injected in the axial direction. Conventional torches work at gas velocities lower than 200 m s^{-1} and maximum temperatures of 10000 K. The power density is about one order of magnitude lower than for DC plasmas and amounts to about 1 kW cm^{-3}. Recently, water-cooled supersonic nozzles have been used at the torch exit to increase the plasma velocities up to Mach 4, reducing the cross-section accordingly. The gases passing the fast alternating electrical field

are excited and mostly dissociated in the case of molecular gases and partially ionized. As in the case of DC plasma jets, the recombination of ionized atoms with free electrons and the recombination to molecules at the nozzle exit results in a hot jet. HF plasma jets have also been used to synthesize diamond coatings and nanosized SiC powders by injecting fine silicon powders and methane.[26] The influence of the plasma composition on the powder structure has also been studied. High-temperature phase α-SiC can be stabilized by adding hydrogen to the sheath gas.[27] However, the application of hydrogen also favours the precursors silicon and methane, which results in a lower efficiency of powder production.

3 EXPERIMENTAL

3.1 DC Plasmajet CVD

For conventional single DC torch experiments, the VPS system A 3000 S from Plasmatechnik with a F4 Sulzer Metco torch is used. A schematic of the process is given in Fig. 1. For injection of the precursors, a nozzle with an inner diameter of 0.4 mm is mounted inside a branched fitting and fine atomization is realized by adding an argon gas stream through the 90° branch. To keep the substrate temperature constant during the coating process, a water-cooled substrate holder is used. To prevent reactions of the precursor with the environment prior to spraying, they are fed to the injector with a peristaltic pump. Toluene is used for cleaning the hoses and the injector.

For emission spectroscopic measurements an optical collimator, which can be moved along an axis covering the distance between nozzle exit and substrate surface, is mounted inside the vacuum chamber. The light is led by an optical fibre to an IfU acousto-optic-spectrometer (AOS). This spectrometer features random wavelength access in less than 1 ms with wavelength resolution of 0.05 nm at 250 nm, and 0.5 nm @ 800 nm. The aperture is about 50 mm^2. The angle between the axes of the sensor and the plasma jet is fixed at 90°.

In addition to the chlorine-containing precursors $SiCl_3CH_3$ and $SiCl(CH_3)_3$, disilanes generated in the Mueller–Rochow synthesis ($(CH_3)_3Si—O—Si(CH_3)_3$) have also been used. Besides silicon wafers, mild carbon steel, austenitic AISI 304 stainless steel, copper, titanium and aluminium alloys have been used as substrates. All substrates are cleaned in an ultrasonic ethanol bath prior to coating. The process parameters are listed in Table 1.

Table 1 Process parameters of the DC Plasmajet CVD experiments

Power (kW)	11.5–17
Argon flow rate (l min^{-1})	30–40
Hydrogen flow rate (l min^{-1})	2–3
Chamber pressure (hPa)	50–75
Precursor flow rate (10^{-3} l min^{-1})	10–25
Atomizing gas flow rate (l min^{-1})	2–3
Distance nozzle–substrate (mm)	100–200

The coatings were characterized by scanning electron microscopy (SEM), X-ray diffraction (XRD) and energy-dispersive X-ray (EDX) analysis. The latter method is not suitable for quantitative analysis of elements lighter than fluorine, but qualitative comparisons are possible by calibrating the height of the silicon peak with that of an uncoated silicon wafer.

3.2 Triple torch DC Plasmajet CVD

Two different setups were used for the Triple torch DC Plasmajet CVD investigations. A schematic of the setup for coating deposition is shown in Fig. 2. Three modified torches, type AS-103L from Tekna Plasma Systems, Inc., were used with an inclination of 22° to the CIP. For injection of the precursors into the converging jet a CIP with an inner tube diameter of 0.4 mm was mounted 20 mm below the plane of the torch exits. The flow of the precursor was controlled by a metering valve, which restricted flow into the low-pressure chamber environment. Both the plasma gases and the atomizing gases were mass flow controlled and premixed in cylindrical chambers before they were injected. Mixtures of argon and hydrogen or nitrogen were used as plasma gases and for atomization. A rotating, water-cooled substrate holder allowed the substrate temperature to be kept constant. The rotational speed was 50 rpm and the cooling water flow was 8.7 l min^{-1}. A single-colour pyrometer, Raytek Marathon ($\lambda = 1.6$ μm), was used to monitor the substrate temperature. To reduce the oxygen content in the chamber, a two-stage rotary vane pump (Leybold Trivac D8A) was used to evacuate the chamber prior to the deposition process. During deposition a liquid ring pump with

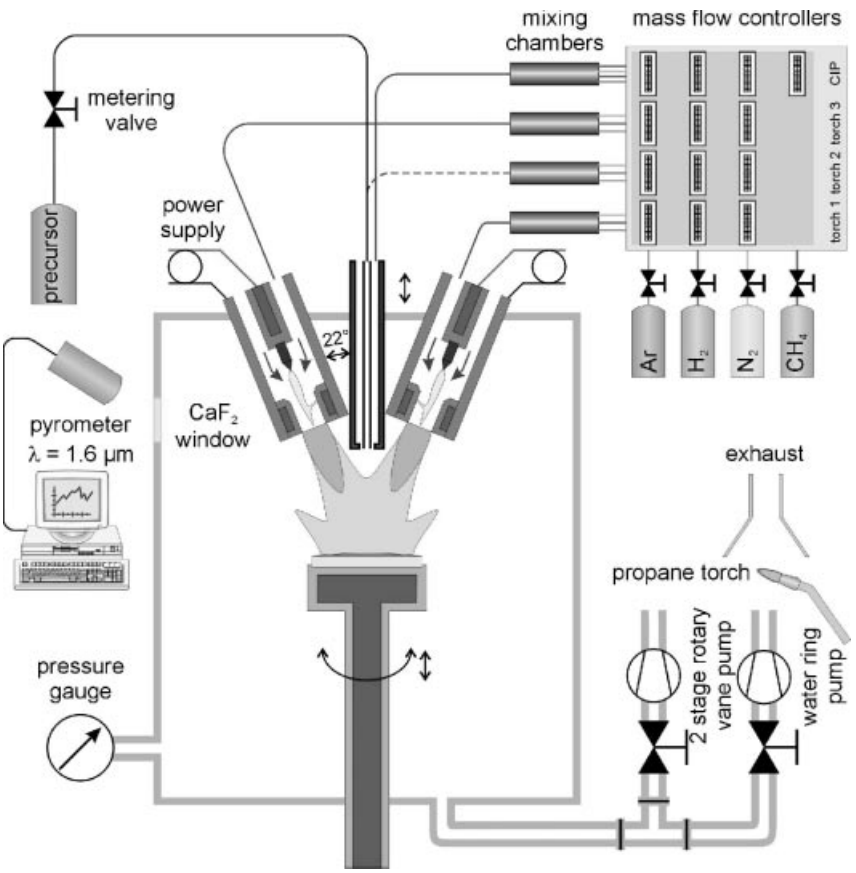

Figure 2 System schematic of the triple torch DC Plasmajet CVD process setup.

a propane torch was applied to burn combustible exhaust gases in the exhaust line.

Hexamethyldisiloxane (HMDSO), hexamethyldisilazane (HMDSZ) and tetramethyldisiloxane (TMDSO) were used as precursors. Molybdenum substrates with a thickness of 2.2 mm and mild steel substrates with a thickness of 3.2 mm were ground in several steps with a final SiC polish with 22 µm size grit and cleaned in an ultrasonic hexane bath before they were coated. After igniting the plasmas the substrates were moved to a stationary distance from the torches and precursor feeding was started when a constant substrate temperature had been achieved. The process parameters are given in Table 2.

Torches manufactured at the University of Minnesota were used for the enthalpy probe studies. The angle between the torches and the CIP was 28°. CIPs with outer diameters of the inner tube of 1 and 2 mm were used to study the influence of the velocity of the atomizing gas at constant flow rates. The CIP was mounted in the plane of the torch exits. Mixtures of argon, hydrogen and nitrogen were used both for plasma and CIP gases. A liquid ring pump kept the chamber pressure constant during the measurements.

Table 2 Process parameters of the triple torch DC Plasmajet CVD experiments

Plasma current (A)	200–375
Argon flow rate per torch (l min^{-1})	25
Hydrogen flow rate per torch (l min^{-1})	0–1
Nitrogen flow rate per torch (l min^{-1})	0–3
Chamber pressure (hPa)	90–930
Precursor flow rate (ml min^{-1})	~0.1
Atomizing gas flow rate (l min^{-1})	2–15
Distance nozzle–substrate (mm)	40–95
Deposition time (min)	5–10
Post-treatment time (min)	0–6

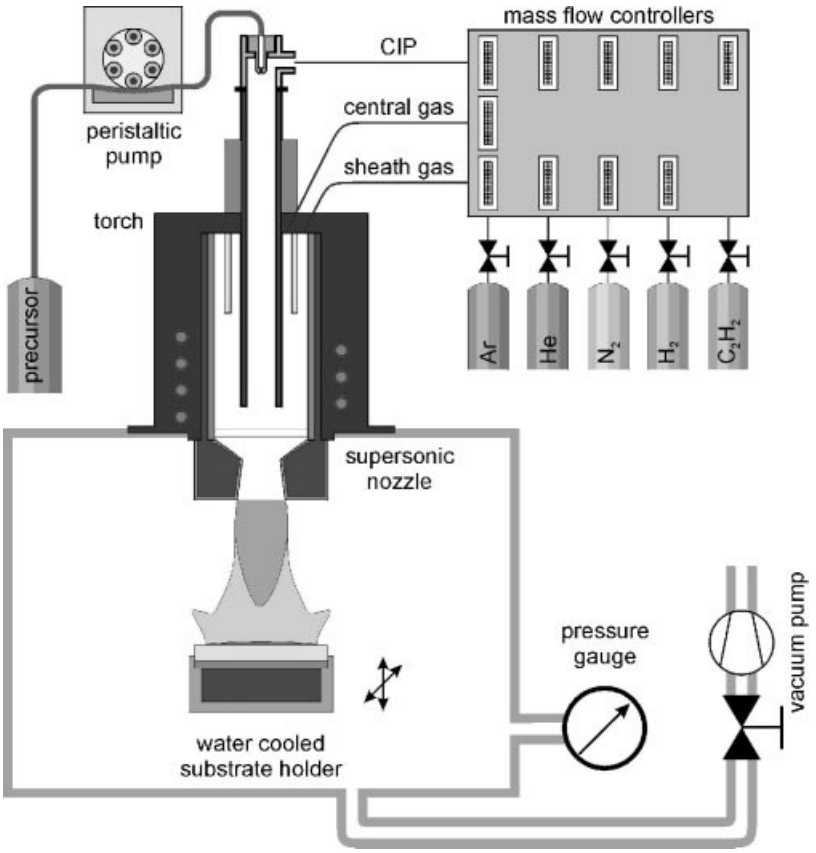

Figure 3 System schematic of the HF Plasmajet CVD process setup.

The coatings were characterized by SEM, XRD and EDX analysis. The latter method is not suitable for quantitative analysis of elements lighter than fluorine.

3.3 HF Plasmajet CVD

For HF Plasmajet CVD investigations, PL35-type torches with Mach 1.5 supersonic nozzles from Tekna Plasma Systems Inc. were used. A scheme of the setup is given in Fig. 3. The precursors were injected into the CIP of the torch by the injector that had also been applied for conventional DC Plasmajet CVD investigations. The precursors were fed by a peristaltic pump to avoid reactions with the environment; the flow rate was kept constant at 0.5 ml min^{-1}. Only argon was used for the central gas; however, mixtures of argon, hydrogen and nitrogen were used for the sheath gas, and argon, helium, nitrogen and acetylene were used for the atomization of the precursor. All gas flows were mass flow controlled. The substrate temperature was kept constant by direct backside water cooling of the substrates or by applying an intermediate 1 mm thickness stainless steel plate. The cooling water flow was 13.4 l min^{-1}. Graphite substrates were not cooled, but rotated at 15 rpm. During the deposition process a liquid ring pump with a propane torch was used to burn combustible exhaust gases in the exhaust line.

The precursors HMDSO, HMDSZ and TMDSO were tested. The surfaces of the mild carbon steel, stainless steel AISI 304, copper, brass and aluminium specimens ($75 \times 75\ mm^2$) with a thickness of 4 mm were milled and ground with a final SiC polish with 37 μm size grit. Additionally, APS-molybdenum-coated stainless steel and aluminium substrates with different surface preparation treatments were tested. The APS-molybdenum coatings were coated in the as-sprayed

Table 3 Process parameters for HF Plasmajet CVD experiments

Plate power (kW)	32.5–59
Sheath gas flow rate (l min^{-1})	
argon	0–55
hydrogen	0–5
nitrogen	0–53
Central gas flow rate (l min^{-1})	
argon	20–27
Atomizing gas flow rate (l min^{-1})	
argon	0–15
nitrogen	0–12
helium	0–15
acetylene	0–0.4
Chamber pressure (hPa)	95–140
Distance nozzle –substrate (mm)	100–110
Deposition time (min)	2.5–12
Post treatment time (min)	0–6

state, brushed with a steel brush and ground with a final SiC polish with 37 μm size grit. All metallic substrates were cleaned in an ultrasonic ethanol bath prior to deposition. Graphite rods with a diameter of 25 mm were used without any surface treatment. After igniting the plasma, the substrates were placed under the torch and the precursor feed was started. The process parameters are given in Table 3.

The coatings were characterized by SEM and EDX analysis. The latter method is not suitable for quantitative analysis of elements lighter than fluorine.

4 RESULTS

4.1 DC Plasmajet CVD

4.1.1 Process characterization

By scanning the UV and visible wavelength range at different positions in the plasma jet, species in the plasma gas (argon and hydrogen) and species resulting from dissociation of the precursors (atomic silicon and carbon, and molecular C_2) were detected. The presence of other species cannot be verified at any location in the plasma jet and for all variations of the process parameters.

The relative concentration distribution of excited species depending on the distance from the nozzle exit is deduced from the intensity of characteristic wavelengths (carbon at 247.9 nm, silicon at 250.7, 263.1 and 390.5 nm, C_2 at 471.5 and 513.0 nm, Hγ at 434.0 nm, argon at 763.5 nm). In order to avoid an influence of the lateral expansion of the jet and different diffusivities of the respective species, the lateral jet profile was recorded and the area under the curve was integrated.

Figure 4 shows a comparison of the intensities of the species detected in the visible range of wavelengths normalized in a logarithmic plot as a function of the distance from the nozzle exit for a free expanding jet and during a coating process. The density of excited plasma gas species decreases from the nozzle exit onwards, whereas the density of excited precursor species increases to a maximum, before an exponential decay occurs. The decay is much steeper when a substrate hinders the

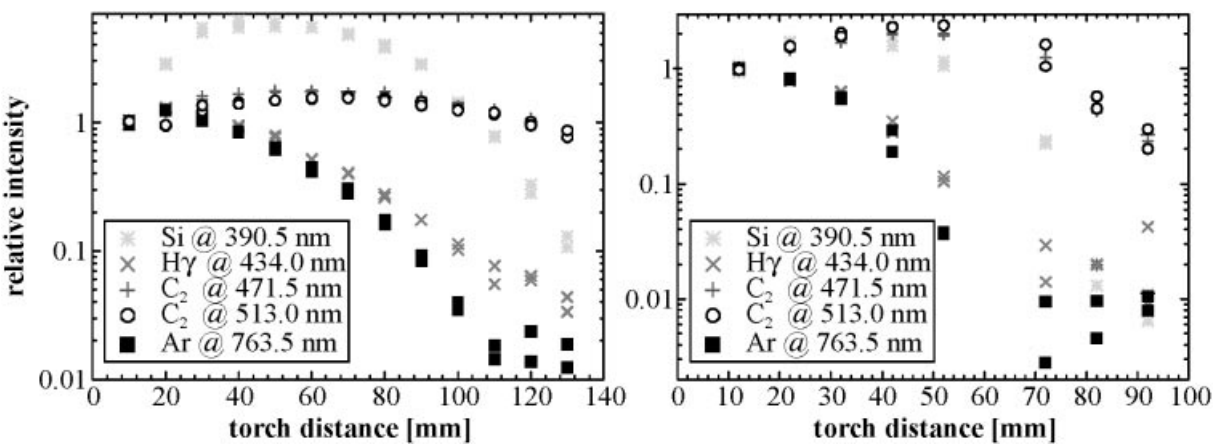

Figure 4 Comparison of the relative density of excited species in a free expanding plasma jet (left) and during the coating process (right): $I = 400$ A; $V'_{Ar} = 35$ l min^{-1}; $V'_{H2} = 2$ l min^{-1}; $V'_{Ar,at} = 2$ l min^{-1}; $V'_{Prec} = 10$ ml min^{-1}; $p = 70$ hPa.

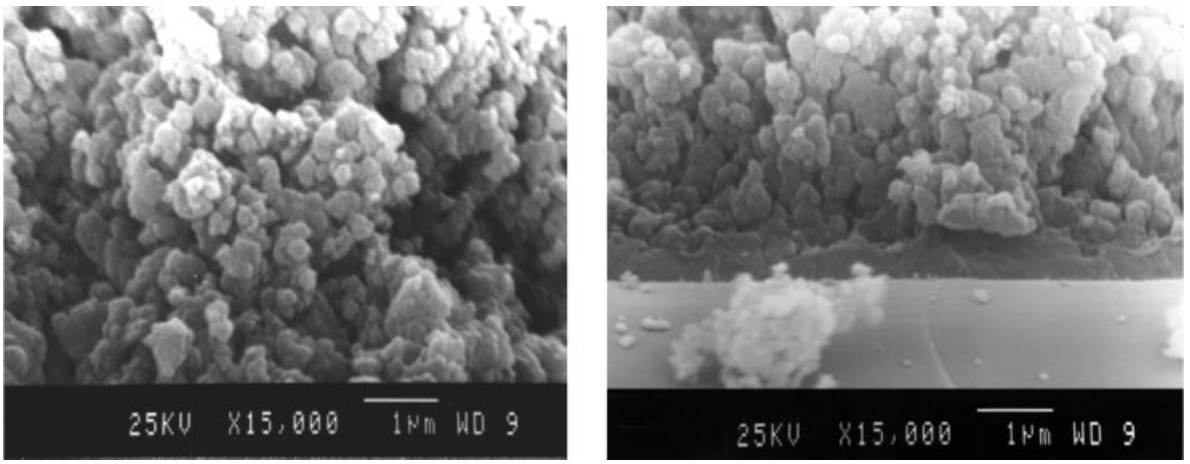

Figure 5 SEM images of fracture surfaces of coatings synthesized from trimethylchlorosilane on silicon wafers. Left: $P = 14.5$ kW, $d = 160$ mm, $V'_{cool} = 1.4$ l min^{-1}; right: $P = 14.5$ kW, $d = 100$ mm, $V'_{cool} = 5.5$ l min^{-1}.

free expansion of the plasma jet and the maximum of excited species is drawn to closer distances from the nozzle, because the velocity of the gases is decreased. For the typical process parameters used in this study the density of excited silicon and carbon atoms approaching the substrate surface is less than 1% of the maximum at about 40 mm from the nozzle exit. For steel substrates, the minimum distance to the nozzle exit is 100 mm for the plasma parameters applied to avoid melting.

4.1.2 Coating morphology

Most coatings show a 'cauliflower' morphology, which means that the coatings are built up by a loose adhesion of nanosized particles on the substrate surface and subsequent coagulation. Figure 5 shows the fracture surfaces of such coatings. The size of the particles depends on the process parameters, but is always smaller than 500 nm. The distance between torch and substrate has a significant influence on the particles size. An increase from 100 to 160 mm causes an increase of the particle size from 50–100 nm to 200–300 nm. The plasma power has no strong influence, either on the particle size or on the deposition rate ($d' = 120$ μm h^{-1} at $P = 11.5$ kW; $d' = 100$ μm h^{-1} at $P = 14.5$ kW).

When the substrate temperature is high enough, dense morphologies can be achieved. The right SEM picture in Fig. 5 shows the fracture surface of a coating synthesized on a silicon wafer in the area of the plasma axis at accordingly high temperatures. In the beginning of the process a 1 μm thick dense morphology is deposited, followed by the cauliflower morphology. Outside the plasma axis, at colder locations, the cauliflower morphology starts at the substrate surface. No influence of the choice of chlorine-containing precursors can be observed. If the particle temperature is sufficiently high, sintering allows compaction, but the shrinkage causes cracks inside the coating. The higher the mismatch of the thermal expansion coefficient of coating and substrate, the higher the tendency for crack formation during the cooling due to residual stresses. On AISI 304 stainless steel and on copper, no crack-free coatings could be synthesized.

The application of chlorine-containing precursors to coating mild carbon steel is problematic, because chlorine impurities inside the coatings cause strong corrosion of the substrate. Consequently, initially strongly adhering coatings peel off the steel substrates within 1 day. The detached coatings show good cohesive strength and flexibility, as no damage is detected for bending angles up to 45°. The deposition rates for these coatings are 1300 μm h^{-1}.

The chlorine-free precursor HMDSO is also suitable for the deposition of coatings with deposition rates up to 1500 μm h^{-1}. Like the chlorine-containing precursors, most coatings show a cauliflower morphology with a maximum particle diameter of 300 nm. Figure 6 shows SEM images of cross-sections of coatings synthesized on an Al–Mg 1.5 alloy and on titanium.

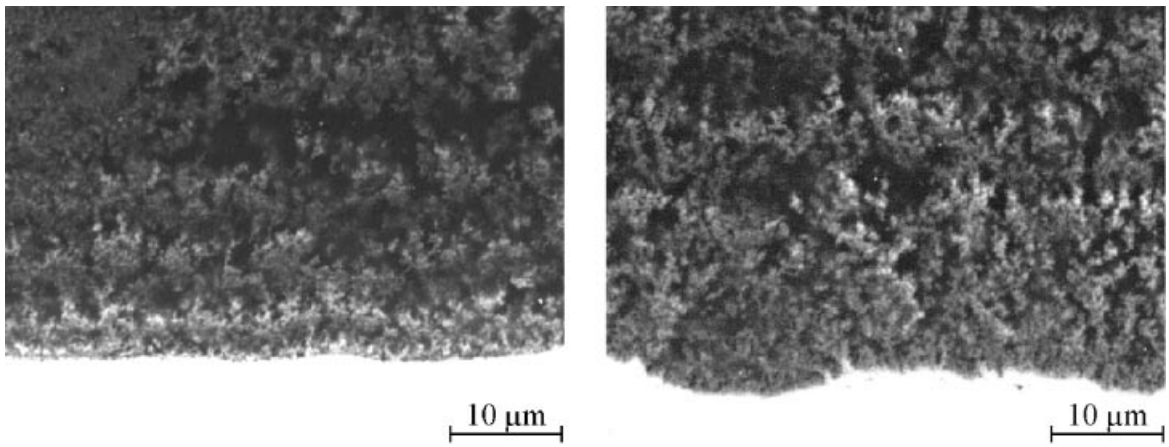

Figure 6 SEM images of cross-sections of coatings synthesized from HMDSO on Al–Mg 1.5 (left: $P = 13$ kW, $d = 120$ mm, $V'_{cool} = 2.0\,l\,min^{-1}$) and titanium (right: $P = 13$ kW, $d = 120$ mm, $V'_{cool} = 2.0\,l\,min^{-1}$).

4.1.3 Coating structure

For all coatings synthesized from chlorine-containing precursors, impurities of at least 3 at.% chlorine are detected by EDX analysis. In some cases the chlorine content at the coating surface is much higher than at the interface with the substrate, which indicates that the deposition conditions changed during the coating process. Additionally, oxygen is detected in coatings from both chlorine-containing precursors and from HMDSO (Fig. 7). The HMDSO precursor contains oxygen, but for the chlorine-containing precursors it must be entrained from the chamber environment or be the result of a post-process reaction. The first is possible, as the chamber is only evacuated to a pressure of 0.01 kPa prior to the deposition and there is always a small leak through the seals of the chamber doors. The latter is also possible, when the chamber is brought to atmospheric pressure, while the coating is still hot enough to react with the incoming air. Finally, water absorption, which is also known from the production of SiC powder,[28] can cause the inclusion of oxygen. The oxygen content in coatings from HMDSO is usually smaller than for coatings from chlorine-containing precursors. Because the coatings cool down rapidly because of the water cooling, it is most probable that the oxygen is due to water absorption and leaks in the chamber.

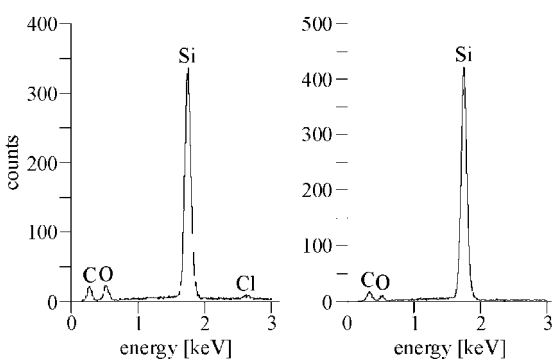

Figure 7 EDX spectra of coatings synthesized from $Si(CH_3)_3Cl$ (left) and HMDSO (right).

The coatings synthesized show two different structures. On the one hand, X-ray amorphous coatings are synthesized, as indicated by a broad band at low diffraction angles. On the other hand, coatings with a crystalline content are obtained. The main crystalline phase is β-SiC (Fig. 8). The broadening of the reflection peak at $2\theta = 35.3°$, i.e. the (111) reflection of β-SiC (3C), allows an estimation for the crystallite size of 5 nm using the Scherrer formula. In some cases, if the $Si(CH_3)_3Cl$ precursor is used, β-SiC and additional peaks that can be assigned to the presence of graphite are detected. The formation of graphite can be attributed to the excess carbon in the precursor.

4.2 Triple torch DC Plasmajet CVD

4.2.1 Process characterization

To characterize the different plasma jet conditions, enthalpy probe measurements were carried out. The influence of the chamber pressure, plasma power, gas composition, and of the injection of different gases through the CIP were investigated. The

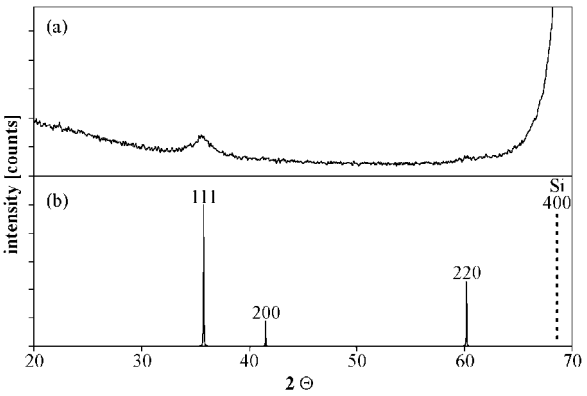

Figure 8 XRD diagram of a coating synthesized from $Si(CH_3)_3Cl$ ($P = 14.5$ kW, $d = 160$ mm, $V'_{cool} = 1.4\ l\ min^{-1}$) in comparison with the theoretical pattern of β-SiC.

temperature and velocity profile along an axis through the centre point of the converging jets and the torch on the right side (positive x-position values) is shown in Fig. 9. The plasma gas is an argon–nitrogen mixture and no atomizing gas flows through the CIP.

The approximate diameter of the converging jet region is 30 mm. Depending on the process parameters, after the coalescence a broadening of the jet occurs. As for a single plasma jet, the axial temperature gradient is significantly smaller than the radial gradient. At the jet boundary, the radial gradient is especially steep for pure argon plasmas. Additions of both nitrogen and hydrogen result in a smoother lateral temperature gradient, which can be attributed to the higher diffusivity and thermal conductivity of atomic nitrogen and hydrogen.

In general, the use of an atomizing gas through the CIP results in cooling of the converging plasma jets and in turbulence, which is indicated by increased fluctuations of the values measured. The cooling effect is especially strong for the injection of hydrogen, because of its high specific heat. The addition of nitrogen to argon as plasma gas can equalize the heat loss resulting from cold gas injection through the CIP at constant plasma current and accordingly increased plasma power. To achieve the same increase of temperature and velocity of the plasma jet the flow rate of added nitrogen has to be significantly higher than for hydrogen addition. For both additions the heat flux to the enthalpy probe increases more significantly than the local mean temperature of the plasma jet. This means that the heat transfer to a substrate cannot directly be derived separate from the local temperature measurements with an enthalpy probe.

4.2.2 Coating morphology

The coatings produced by triple torch DC Plasmajet CVD show good homogeneity, which can be attributed to the rotation of the substrate. Most coating surfaces show a topology of microsized rounded constituents (Fig. 10), but smooth surfaces are also synthesized. The size of the rounded constituents decreases from the plasma axis to the boundary of the coatings. In some cases columnar structures are observed, which indicate that the coating grows in columns. The pillars evolve when a column starts to grow preferentially, which can

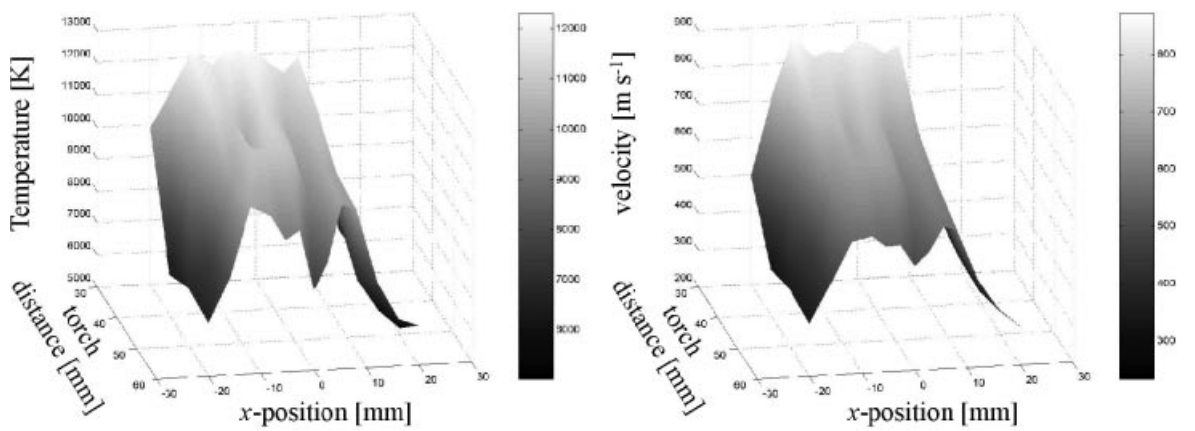

Figure 9 Temperature and velocity profiles of an argon/nitrogen plasma: pressure: 400 hPa; Ar flow rate: $20\ l\ min^{-1}$/torch; N_2 flow rate: $2.2\ l\ min^{-1}$/torch. Torches 1–3: $U = 41.5$ V, $I = 250$ A, $P = 10.4$ kW.

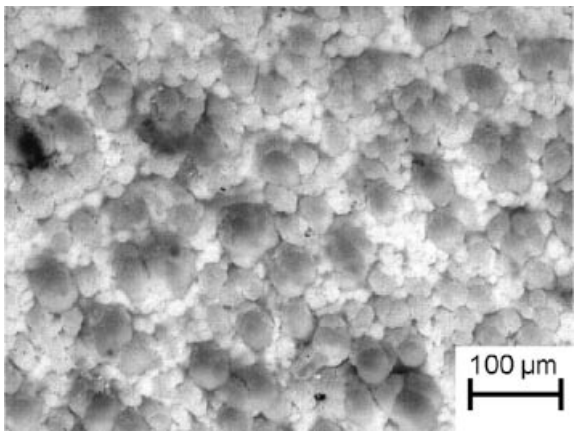

Figure 10 Optical microscope image of the surface of a triple torch DC Plasmajet CVD coating from HMDSO.

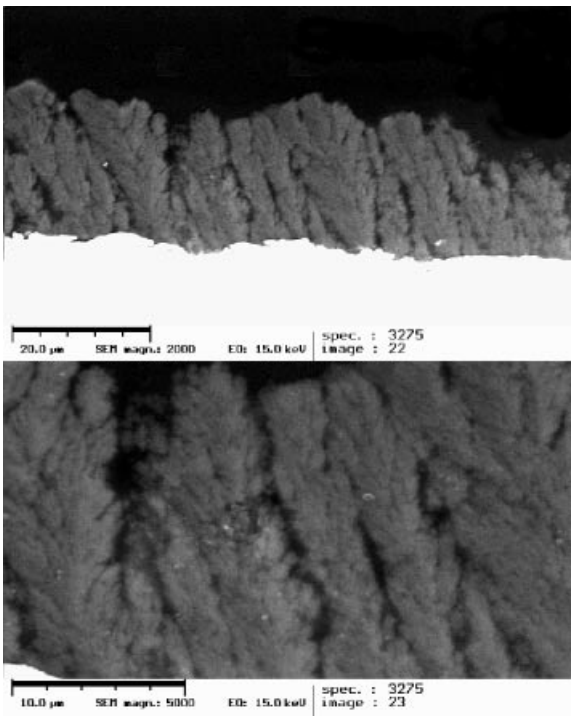

Figure 11 SEM images of cross-sections of a triple torch DC Plasmajet CVD coating from TMDSO with columnar morphology. Plasma gases: Ar, 25 l min^{-1}, N_2, 2 l min^{-1}; atomizing gas: CH_4, 1 l min^{-1}; plasma current: 325 A; precursor: TMDSO; torch distance: 50 mm; pressure: 90 hPa; deposition time: 3 min; post-treatment time: 2 min.

start as a statistical process. The decreased distance to the torches can cause improved deposition conditions and lead to a further increase in the deposition rate, and thereby to the formation of columns.

The lateral gradient of the substrate temperature and of the density of species approaching the substrate surface causes changes in the coatings morphology. First the size of columns decreases, which can be attributed to an increased density of nuclei on the substrate surface at lower temperatures. At the edge of the coating the substrate temperature is usually too low to allow good adherence of the coating. In these areas the coating can easily be removed by a paper towel, whereas the rest of the coating resists scratching with a tungsten stencil much better than all the other substrates that have been used. When pure argon plasmas are used, high currents must be applied to achieve sufficient heat transfer to the substrate.

SEM investigations confirm the above-mentioned assumption of a columnar morphology for most coatings synthesized. One example is given at two different magnifications in Fig. 11. The columns show an inclination to the axis of the united plasma jet, which can be attributed to the increased density of growth species in this area. At high magnifications, in some coatings, single nanosized particles that have been built into the morphology of the coating can be detected. However, they constitute a negligible fraction of the deposit. The coatings with smooth surfaces show a microporous morphology near the surface, but a columnar morphology underneath. The individual columns have grown together to form a dense surface that does not allow penetration of the coating by a resin; this makes the preparation of cross-sections very difficult, but means there is good potential for corrosion protection.

Depending on the process parameters, deposition rates between 300 and 1200 µm h^{-1} are obtained. An influence of the precursor type on the deposition rate cannot be observed.

4.2.3 Coating structure

The coating structure depends strongly on the composition of the plasma and atomizing gas. When mixtures of argon and nitrogen are used as plasma gases, the coatings contain crystalline β-Si_3N_4 and, in some cases, α-Si_3N_4 as well as amorphous phases (Fig. 12). In general, the coatings synthesized with pure argon or mixtures of argon and hydrogen as plasma gases result in completely X-ray amorphous coatings. Peaks that

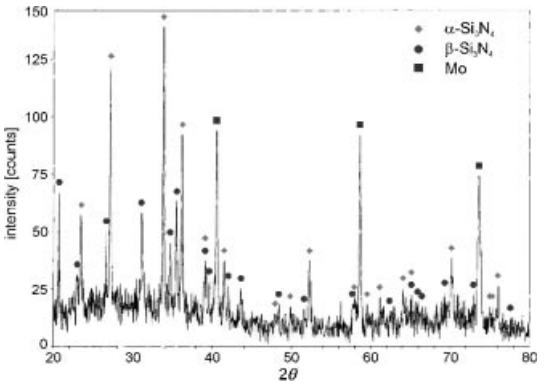

Figure 12 XRD diagram of a triple torch DC Plasmajet CVD coating from HMDSO. Plasma gases: Ar, 25 l min^{-1}, N_2, 2 l min^{-1}; atomizing gas: N_2, 2 l min^{-1}; plasma current: 300 A; precursor: HMDSO; torch distance: 60 mm; pressure: 90 hPa; deposition time: 5 min.

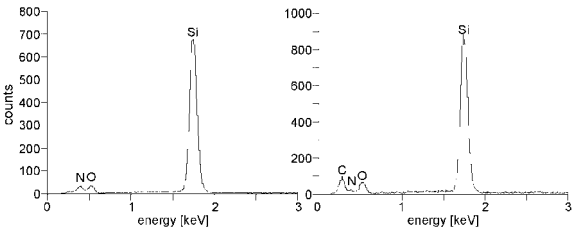

Figure 13 EDX spectra of point measurements on a coating synthesized from HMDSZ. Plasma gas: Ar, 25 l min^{-1}; atomizing gas: Ar, 7.5 l min^{-1}; plasma current: 375 A; precursor: HMDSZ; torch distance: 50 mm; pressure: 90 hPa; deposition time: 3 min; post-treatment time: 2 min.

can be attributed to β-SiC (3C) are detected in some cases, but the diffraction pattern never matches the theoretical pattern perfectly. This may result from the columnar morphology of the coatings, which can lead to suppression of peaks when only certain crystal orientations grow on the surface.

Some mild-steel substrates, which are coated without addition of hydrogen to argon as plasma gas, are oxidized. The corresponding XRD patterns show various iron oxides with stoichiometry Fe_2O_3 and/or Fe_3O_4. On the other hand, the use of hydrogen as the plasma gas results in etching of the steel surface. The etching effect is easily detectable, because the etching rate at the grain boundaries is significantly higher than for the grains themselves. Because of the mismatch of thermal expansion, coatings synthesized on steel substrates often peel off due to residual stresses. The peeling is strongest in the area of highest substrate temperature and highest coating thickness, i.e. the plasma axis. When the coating has peeled from the substrate, the grain structure of the substrate is clearly visible. The high substrate temperature with strong radial temperature gradients results in a grain growth from the centre of the coating in a radial direction. The grain size decreases with increasing distance from the centre. Therefore, the use of hydrogen can help to achieve a clean and active substrate surface, but it has to be controlled in order to avoid damaging the grain boundaries.

EDX analyses show nitrogen, in addition to silicon and carbon, in coatings synthesized from HMDSZ and when nitrogen is applied as plasma or atomizing gas. Additionally, all coatings contain oxygen. As in the case of the coatings synthesized by conventional DC Plasmajet CVD, the oxygen can result from water absorption or from impurities in the chamber environment due to insufficient evacuation or imperfect sealing of the reactor doors.

Some amorphous coatings contain different phases. Figure 13 shows two EDX spectra from different locations in a coating synthesized from HMDSZ in a pure argon plasma. Whereas one phase contains nitrogen but only negligible carbon, the other phase is carbon rich and contains nearly no nitrogen. The contrast due to different chemical compositions of the phases cannot be detected in SEM pictures.

4.3 HF Plasmajet CVD

4.3.1 Process characterization

Like the triple torch DC Plasmajet CVD process, HF Plasmajet CVD was also characterized by enthalpy probe measurements. Temperature and gas velocity along the plasma axis were measured for a constant plate power of 25 kW, a chamber pressure of 130 hPa and various sheath and atomizing gas compositions. Figure 14 shows a comparison of the temperature versus torch distance function for the condition of 21 l min^{-1} argon in the central gas and 40 l min^{-1} in the sheath gas (argon or nitrogen) with and without use of an atomizing gas (nitrogen) flow of 5 l min^{-1}. It is obvious that the use of the atomizing gas causes a drop of the plasma temperature of 1000 K at distances close to the torch exit. Additionally, the temperature drop behind the plateau of nearly constant high values is shifted about 5 mm to shorter torch distances. At distances greater than

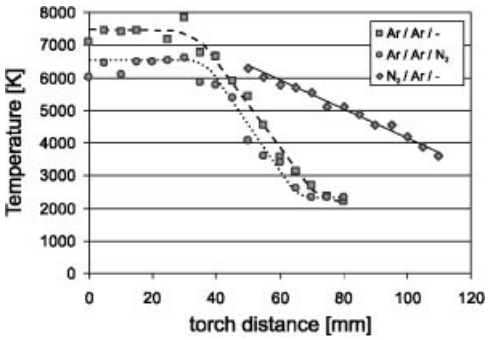

Figure 14 Plasma temperature on the plasma axis as a function of torch distance and gas composition.

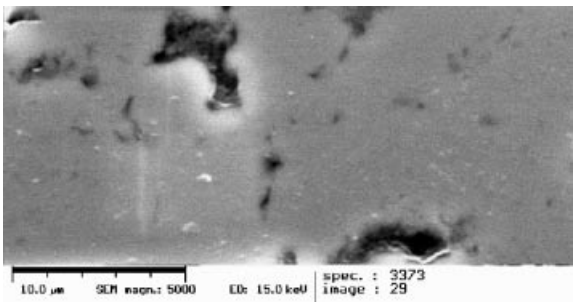

Figure 15 SEM picture of an HF Plasmajet CVD coating synthesized from HMDSO.

70 mm the plasma temperature has decreased so much that accurate measurements are not possible, and the difference between the plasma with and without use of atomizing gas vanishes.

When pure nitrogen is used in the sheath gas, the closest possible torch distance at which measurements can be taken is 50 mm, because the heat flux to the probe reaches a critical value, though the local plasma temperature is far below values that can be measured for pure argon plasmas. In addition to the increased heat flux, which provides a strong heating of the substrate, nitrogen causes a significant decrease of the temperature gradient compared with pure argon plasmas, which is beneficial for suppressing the formation of nanoparticles. Because of insufficient substrate temperature and high temperature gradients, it is not possible to deposit coatings with good mechanical properties without use of nitrogen in the sheath gas for the range of process parameters used.

4.3.2 Coating morphology

The coatings synthesized show a dense morphology, but contain pores with a size in the range 1–5 µm (Fig. 15). Deposition rates between 500 and 1200 µm h^{-1} are achieved, and the diameter of the coated area reaches up to 50 mm. The thickness distribution is more homogeneous than that of DC Plasmajet CVD coatings, because the gradient of the plasma properties is smaller in the HF Plasmajet. For optimized parameters there is a perfect interface between substrate and coating.

For good adhesion of the coatings, high substrate temperatures are necessary. When the deposition is started without substrate preheating, coatings with good internal mechanical properties can be obtained, but there is no adherence to the substrate, which results in free-standing disks. The best coatings with respect to homogeneity and adhesion to the substrate are synthesized on copper, brass and mild carbon steel. Coatings on X5 Cr Ni 18 10 tend to crack off during cooling, though the coefficient of thermal expansion is lower than that of copper. The melting point of aluminium is too low to allow the deposition of coatings with good mechanical properties.

Graphite can be coated without cooling of the substrate. However, when graphite is heated to a glow, no coating forms; only erosion is observed. In general, the coating shows the same topology as the graphite substrate. This means that the graphite substrate has to provide a fairly dense surface in order to allow the synthesis of a coating that covers the complete surface and, therefore, provides wear and oxidation resistance.

For metallic substrates, an influence of the surface preparation is also observed. For substrates with a scale resulting from the fabrication of the sheet material, coatings tend to peel off. Machined, polished and thoroughly cleaned surfaces result in the best adhesion. The roughness of the substrate has a significant influence. Coatings on top of as-sprayed APS molybdenum coatings peel off completely. Coating adhesion is improved by removing the oxide scale with a steel brush. Further planarization of the surface by polishing allows deposition of coatings without any spalling.

5 SUMMARY AND DISCUSSION

The triple torch Plasmajet CVD process produces Si–C(–N) coatings with improved properties, compared with those produced by conventional

DC Plasmajet CVD, when liquid precursors HMDSO, TMDSO or HMDSZ are used. This can be attributed to the axial injection further downstream compared with the case of the conventional DC Plasmajet process. In combination with the decreased flow rate of the precursor, the precursor species form a less supersaturated vapour and undergo a less steep temperature gradient. In combination with the improved homogeneity of the species distribution due to the axial injection, a suppression of the formation of nanoparticles is achieved. Columnar coatings can only be applied for corrosion and oxidation protection if the columns have formed a dense surface by growing together.

To achieve good adhesion of the coatings the substrate needs to be heated to a material-specific temperature prior to precursor injection. There is also a maximum substrate temperature for the deposition of coatings. Substrate materials with a high melting temperature can be overheated. The higher the substrate temperature, the lower is the density of nuclei on the substrate surface, and thereby the lower the density of columns and the larger the size of the columns and the higher the surface roughness, as the columns form rounded heads during the deposition process.

In general, substrates with a low thermal expansion mismatch compared with the coating exhibit less spalling of the coating. However, there is a further influence of the substrate material, as stainless steel shows worse adhesion than copper or brass, though its thermal expansion is closer to Si–C–N. A possible explanation might be that copper forms neither carbides nor silicides, in contrast to iron, and, therefore, allows a catalytic reaction on its surface, which is beneficial for the homogeneity of nucleus formation and thereby of the complete coating.

As HF plasmas feature a larger diameter and lower temperature gradients compared with DC plasmas, larger areas can be coated with a homogeneous thickness distribution and constant mechanical properties. Additionally, impurities arising from electrode material in the coatings are avoided.

Depending on the process parameters, the Plasmajet CVD processes can be used for both production of nanosized powders and for coatings with columnar or dense morphology. The application of nitrogen as plasma gas results in the deposition of coatings with at least a fraction of crystalline Si_3N_4. The crystallization of SiC is suppressed compared with that of Si_3N_4. By rotating the substrate the homogeneity of the coating is improved.

In general, all Plasmajet CVD processes have proven to be suitable for the deposition of Si–C–N coatings with deposition rates exceeding 1000 μm h^{-1}, which qualifies them for industrial applications in the field of wear, corrosion and/or oxidation protection. However, the processes are restricted to rather simple substrate geometries (small plane plates or cylindrical rods or tubes), because of the necessity for a homogeneous substrate temperature distribution and the distance between the torch and substrate.

Acknowledgements The results presented are partially funded by the Deutsche Forschungsgemeinschaft within the limits of the compound project 'New precursor ceramics from condensed precursors by DC- and HF-plasmas' (SPP 1037, Wi 1509/2). The authors would like to thank Wacker Chemie Germany for providing the precursors HMDSO, HMDSZ and TMDSO. Further thanks are also due to Alexander Schwenk (TU Ilmenau) for assistance during the enthalpy probe measurements in Sherbrooke.

REFERENCES

1. Novikov NV, Voronkin MA, Zaika NI. *Diamond Relat. Mater.* 1992; **1**: 580.
2. Lelogeais M, Ducarrior M. *Surf. Coat. Technol.* 1991; **48**: 121.
3. Ducarroir M, Lartigue JF, Morancho R, Bastin G. *C. R. Acad. Sci. Paris* 1998; **307**(II): 541.
4. Lartigue JF, Ducarroir M, Armas B. *Proceedings of 9th International Conference on CVD*. Electrochemical Society: Pennington, NJ, 1984; 561.
5. Maury F, Hatin Z, Biran C, Birot M, Dunogues J, Morancho R. *Proceedings of 6th European Conference on CVD*. Iscar: Jerusalem, 1987; 390.
6. Maury F, Hatin Z, Reynes A, Morancho R. *Proceedings of 10th International Conference on CVD*. Electrochemical Society: Pennington, NJ, 1987; 1080.
7. Wickramanayaka S, Hatanaka Y, Nakanishi Y, Wrobel AM. *J. Electrochem. Soc.* 1994; **141**: 2910.
8. Windischmann H. *J. Vac. Sci. Technol. A* 1991; **9**: 2459.
9. Lelogeais M, Ducarrior M. *Surf. Coat. Technol.* 1991; **48**: 121.
10. Klumpp A, Schaber U, Offereins HL, Kühl K, Sandmaier H. *Sens. Actuators A* 1994; **41–42**: 310.
11. Zhang W, Zhang K, Wang B. *Mater. Sci. Eng. B* 1994; **26**: 133.
12. Gerretsen J, Kirchner G, Kelly T, Mernagh V, Koekoek R, McDonnell L. *Surf. Coat. Technol.* 1993; **60**: 566.
13. Manfredotti C, Fizotti F, Osenga C, Amato G, Boarino L. *Physica A* 1993; **135**: 191.

14. Cauchetier M, Croix O, Luce M, Baraton MI, Merle T, Quintard P. *J. Eur. Ceram. Soc.* 1991; **8**: 215.
15. Suzuki M, Maniette Y, Nakata Y, Okutani T. *Ceram. Int.* 1993; **19**: 407.
16. Yali L, Yong L, Fen Z, Zhuangqi H. *Mater. Sci. Eng. A* 1994; **A174**: L23.
17. Suzuki M, Maniette Y, Nakata Y, Okutani T. *J. Am. Ceram. Soc.* 1993; **76**: 1195.
18. Martinengo H, Musset E, Herlin N, Armand X, Luce M, Cauchetier M, Roulet H, Gheorghiu A, Dufour G, Senemaud C. *Silicates Industriels* 1996; **61**: 9.
19. Görke O, Schubert H. Presentation at the status conference of the DFG SPP on precursor ceramics, Darmstadt, Germany, March 15, 2000, TU Berlin.
20. Kojima Y, Andoo Y, Doi M. *Iron Steel Inst. J. Int.* 1995; **35**: 1381.
21. Ohtake N, Yoshikawa M. *New Diamond* 1990; **1**.
22. Singh SK, Stachowicz L, Girshick SL, Pfender E. *J. Mater. Sci. Lett.* 1993; **12**: 659.
23. Eguchi K, Yoshida T. *J. Mater. Sci. Lett.* 1993; **12**: 858.
24. Heberlein J, Rao NP, Neumann A, Blum J, Tymiak N, McMurry PH, Girshick SL. *Thermal Spray: A United Forum for Science & Technology Advances*. ASM International: Materials Park, OH, USA, 1997; 329–333.
25. Tymiak N, Iordanoglou DI, Neumann D, Gidwani A, Di Fonzo F, Fan MH, Rao NP, Gerberich WW, McMurry PH, Heberlein JVR, Girshick SL. Proceedings of the 14th ISPC, Prague, Czech Republic, 1999; 1989–1994.
26. Guo JY, Gitzhofer F, Boulos MI. *J. Mater. Sci.* 1995; **30**: 5589.
27. Guo JY, Gitzhofer F, Boulos MI. *Plasma Chem. Plasma Process*. 1997; **17**: 219.
28. Zhu CW, Zhao GY, Revankar V, Hlavacek V. *J. Mater. Sci.* 1993; **28**: 659.

